

Oxidation parameters determination of Cu–Al–Ni–Fe shape-memory alloy at high temperatures

Mediha Kök · Koksal Yildiz

Received: 4 January 2014 / Accepted: 16 March 2014 / Published online: 1 April 2014
© Springer-Verlag Berlin Heidelberg 2014

Abstract In this study, isothermal oxidation behavior of a Cu–Al–Ni–Fe shape-memory alloy between 500 and 900 °C was investigated. Alloy samples were exposed to oxygen by TG/DTA for 1 h at a constant temperature, allowing for calculation of the oxidation constant and activation energy values of the oxidation process. The oxidation constant value increased with temperature, reaching saturation at 800 °C. The effect of oxidation on crystal structure, surface morphology and chemical composition of the Cu–Al–Ni–Fe alloy was determined by X-ray diffractometer (XRD) and scanning electron microscope (SEM)–energy-dispersive X-ray (EDX) analyses. With increasing oxidation temperature, number and intensity of the characteristic 18R martensite phase peaks were reduced while Al₂O₃ phase peaks were increased. In parallel to the XRD results, the same variations were also detected by SEM–EDX measurements.

1 Introduction

In recent years, shape-memory alloys have been drawing significant attention for use as functional smart materials [1]. Shape-memory effect, an important phenomenon closely related with the martensitic transformation, occurs when crystal structure of the material changes. This change in crystal structure depends on the austenite–martensite transformation temperature and deformation [2]. Martensitic transformations are diffusionless first-order solid–solid phase transformations where a high-temperature phase transforms to a low-temperature phase by means of a shear stress [3].

Copper-based shape-memory alloys, such as Cu–Al- and Cu–Zn-based alloys, are attractive materials for practical applications due to their pseudoelasticity and shape-memory effect, offering advantages in electrical and thermal conductivity at a low cost [4]. Among the different copper-based shape-memory alloys, the most well-known systems are Cu–Al–Ni and Cu–Al–Zn alloys. While Cu–Al–Zn alloys are less expensive to produce, Cu–Al–Ni alloys have higher thermal stability and operation temperatures [5]. The high-operating temperature of Cu–Al–Ni-based alloys makes them more advantageous than the other traditional shape-memory alloys. Today, the demand for shape-memory alloys, which can be used as smart materials at temperatures higher than 200 °C, is increasing continuously [6, 7].

It has already well known that most metals have a high tendency for oxidation in oxidative atmospheres, a tendency that increases with increasing temperature [8]. However, presence of high number of components with different oxidation affinities makes the oxidation process more complex in alloys than in pure metals [9]. As the number of oxidation modes increases with increasing number of components, it will be much more difficult to understand the complex oxidation behavior of the quaternary and higher component alloys [10]. It has already been demonstrated that maintaining the stability of the shape-memory effect in shape-memory alloys necessitates a stable microstructure. Surface oxidation caused by long-term exposure to air leads to variation in the surface microstructure of the shape-memory actuators, which in turn leads to diminishing shape-memory effects [11, 12]. For this reason, oxidation resistance of alloys is still widely studied so as to identify potential applications of these alloys at high temperatures in an atmospheric environment [13]. While oxidation does present a certain loss of function, oxidation also offers some advantages as it increases

M. Kök (✉) · K. Yildiz
Department of Physics, Firat University, 23119 Elazig, Turkey
e-mail: msoglu@firat.edu.tr

the wear resistance of the shape-memory alloys [14]. Thus, the oxidation behavior of the shape-memory alloys is quite important for their high-temperature applications and should be investigated carefully. In this study, isothermal oxidation behavior of Cu–13 wt% Al–4 wt% Ni–4 wt% Fe shape-memory alloy at high temperatures (500–900 °C) was investigated. The crystal structures and morphologies of oxidized Cu–Al–Ni–Fe alloy samples were also characterized. This study was aimed to provide insight into high-temperature application behaviors of the increasingly preferred CuAlNiFe alloys.

2 Experimental

2.1 Isothermal oxidation procedure

In this study, Cu–13 wt% Al–4 wt% Ni–4 wt% Fe shape-memory alloy was used to investigate the oxidation behavior. The alloys were produced by arc melter and non-heat-treated samples to which oxidation was to be applied were prepared with $2 \times 2 \times 2$ mm dimensions. Then, they were ground to remove surface roughness. Acetone was used to clean the ground samples. TG/DTA (Perkin Elmer Pyris) was used to apply oxygen at constant temperature to the samples. Samples placed into the TGA/DTA were heated to the required oxidation temperature at a heating rate of 50 °C/min under pure nitrogen atmosphere. In this study, 500, 600, 700, 800 and 900 °C were selected as oxidation temperatures because heat treatment is frequently applied to Cu-based alloys within this temperature range. After being heated to the oxidation temperature in the TGA furnace, the alloy was held at that temperature for 1 h under 100 ml/min flowing oxygen.

2.2 Test measurements

Phase analyses were performed using an XRD (Rigaku RadB-DMAX II) at room temperature so as to observe the variations on the surface of the CuAlNiFe alloy, which had been subjected to oxygen at 500, 600, 700, 800 or 900 °C. Surface morphologies of the oxidized alloy samples were investigated using a scanning electron microscope (SEM, JEOL JSM7600F) at room temperature. To determine the chemical compositions of the oxidized samples, an energy-dispersive X-ray (EDX) spectroscope was used.

3 Results and discussion

3.1 Isothermal oxidation kinetics

In general terms, the increase of the mass of a metal as a result of oxidation can be linear increase or parabolic [15].

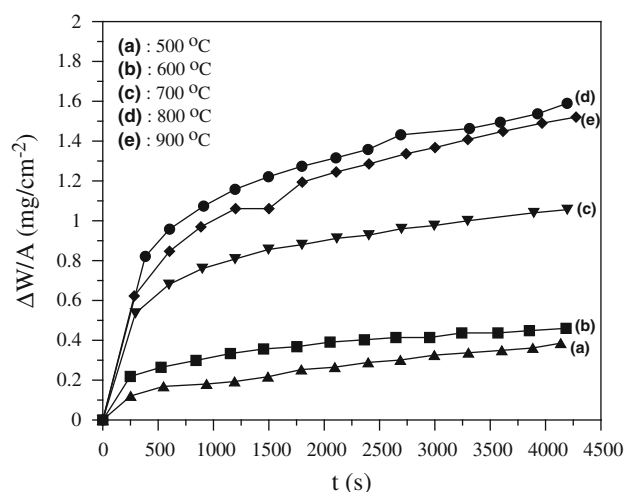


Fig. 1 Mass gain curves of Cu–Al–Ni–Fe shape-memory alloy with oxidation temperatures for 1 h

As seen from Fig. 1, the curve of the mass increase is parabolic. This figure gives information about the mass gain per area at constant temperature. Parabolic isothermal oxidation constant (K_p) was calculated using the equation given below:

$$\left(\frac{\Delta W}{A}\right)^n = K_p t \quad (1)$$

To calculate the parabolic isothermal oxidation constant, n was taken as 2. The slope of the $(\Delta W/A)^2$ vs. (t) graph gives the value of the oxidation constant (K_p). K_p values calculated from the curve of the graph are given in Table 1. As the correlation constant given in the Table 1 is between 0.90 and 0.99, it can be stated that oxidation of CuAlNiFe alloy obeyed the parabolic law [15]. The relationship between isothermal oxidation temperatures vs. K_p is shown in Fig. 2. The oxidation rate of the alloy was the same and so low at 500 and 600 °C; this is common in most of the metals as they are prone to oxidation in oxidizing atmospheres [15], while between 600 and 800 °C, oxidation rate increased notably (Fig. 2). The oxidation constant values calculated for 800 and 900 °C are almost equal, indicating that CuAlNiFe alloy reached its oxygen saturation limit after 800 °C. There are a handful of studies in the literature about the oxidation behavior of CuAlNi- or CuAlNi-based alloys [16–18]. In each of those studies, non-isothermal oxidation behavior was investigated, which only allows for the identification of the amount of oxygen diffused into the surface of the alloy rather than the oxygen constant, which can only be obtained using isothermal methods.

The temperature dependency of K_p can be represented by the following equation:

$$K_p = K_o e^{(E/RT)} \tag{2}$$

Here E represents effective activation energy, T is the oxidation temperature and R is the gas constant. If natural logarithms of both sides are taken [19],

$$\ln(K_p) = \ln(K_o) - E/(RT) \tag{3}$$

Figure 3 shows $\ln(K_p)$ vs. $1/T$ of the CuAlNiFe alloy in oxygen atmosphere. The oxidation constant was 58.66 kJ/mol according to the slope of this curve. Tatar and his co-workers conducted a non-isothermal oxidation study and calculated the activation energy for oxidation of the Cu–Al–Ni and Cu–Al–Ni–Mn shape-memory alloys that were exposed or not exposed to radiation. Activation energy values of alloys which were not exposed to radiation were found to be 29.3 and 56.46 kJ/mol, respectively [16, 17]. When compared with ternary Cu–Al–Ni shape-memory alloy, the higher oxidation energy of the Cu–Al–Ni–Mn alloy could be attributed to the presence of Mn in the structure. In fact, it was emphasized in a previous study that the oxidation of Mn in the Ni–Mn–Ga alloy was high [15]. The activation energy of CuAlNiFe alloy examined in

Table 1 The oxidation constant values of the studied CuAlNiFe alloys between 500 and 900 °C

Temperature (°C)	K_p ($\text{mg}^2 \text{cm}^{-4} \text{s}^{-1}$)	R (correlation coefficient)
500	3.38×10^{-5}	0.99
600	4.39×10^{-5}	0.92
700	2.23×10^{-4}	0.88
800	4.78×10^{-4}	0.92
900	4.91×10^{-4}	0.95

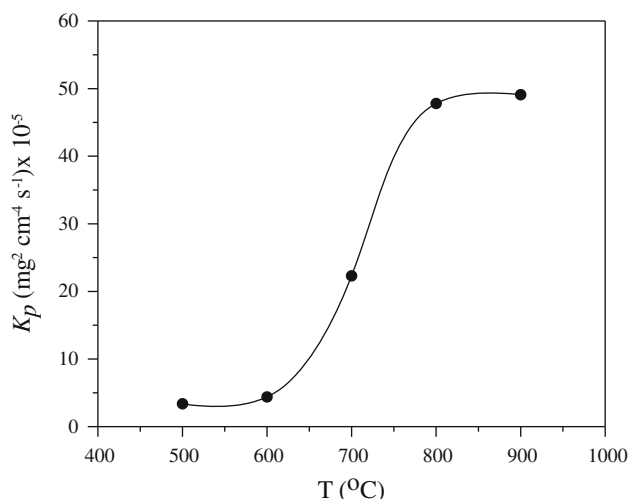


Fig. 2 The variation of oxidation constants of Cu–Al–Ni–Fe alloy with increasing temperature from 500 to 900 °C

this study was relatively higher than Cu–Al–Ni shape-memory alloy, suggesting that the oxidation rate of iron was high. However, if this alloy is compared with NiTi, it can be seen that activation energy of CuAlNiFe was lower. Dagdelen and Ercan found the activation energy value for Ni–45.16 %Ti (atomic) alloy as 65.47 kJ/mol [20]. This was because the oxidation rate of Ti was higher than other elements in NiTi [20].

3.2 Analysis of the crystal structure and surface morphology

To examine the temperature-dependent structural properties of the Cu–Al–Ni–Fe alloy, X-ray diffractometer (XRD)

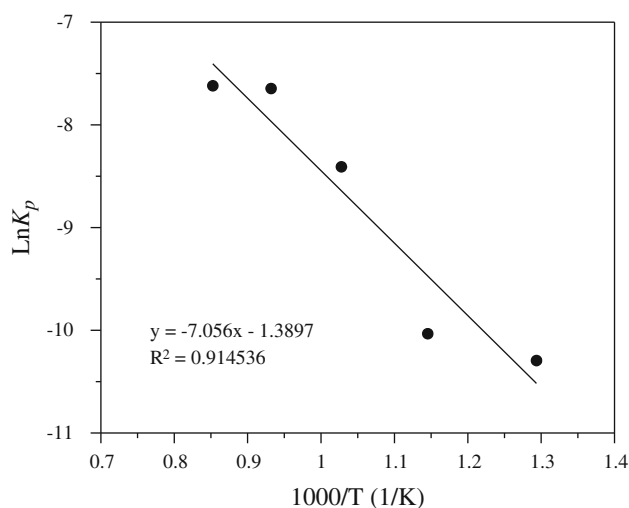


Fig. 3 Oxidation activation energy graph of Cu–Al–Ni–Fe shape-memory alloy

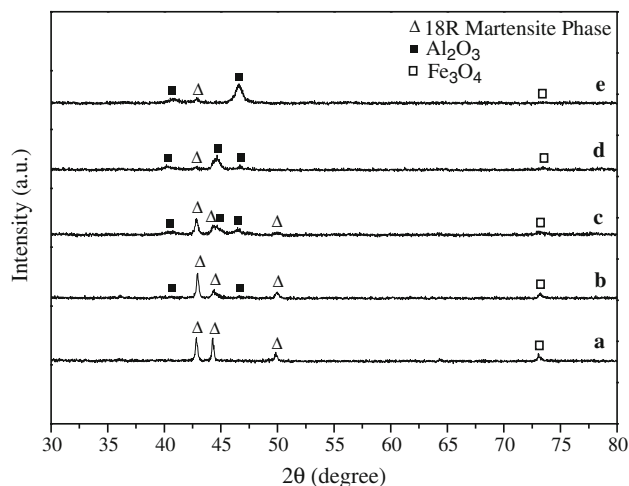


Fig. 4 X-ray patterns of oxidized Cu–Al–Ni–Fe shape-memory alloy at, a 500 °C, b 600 °C, c 700 °C, d 800 °C and e 900 °C

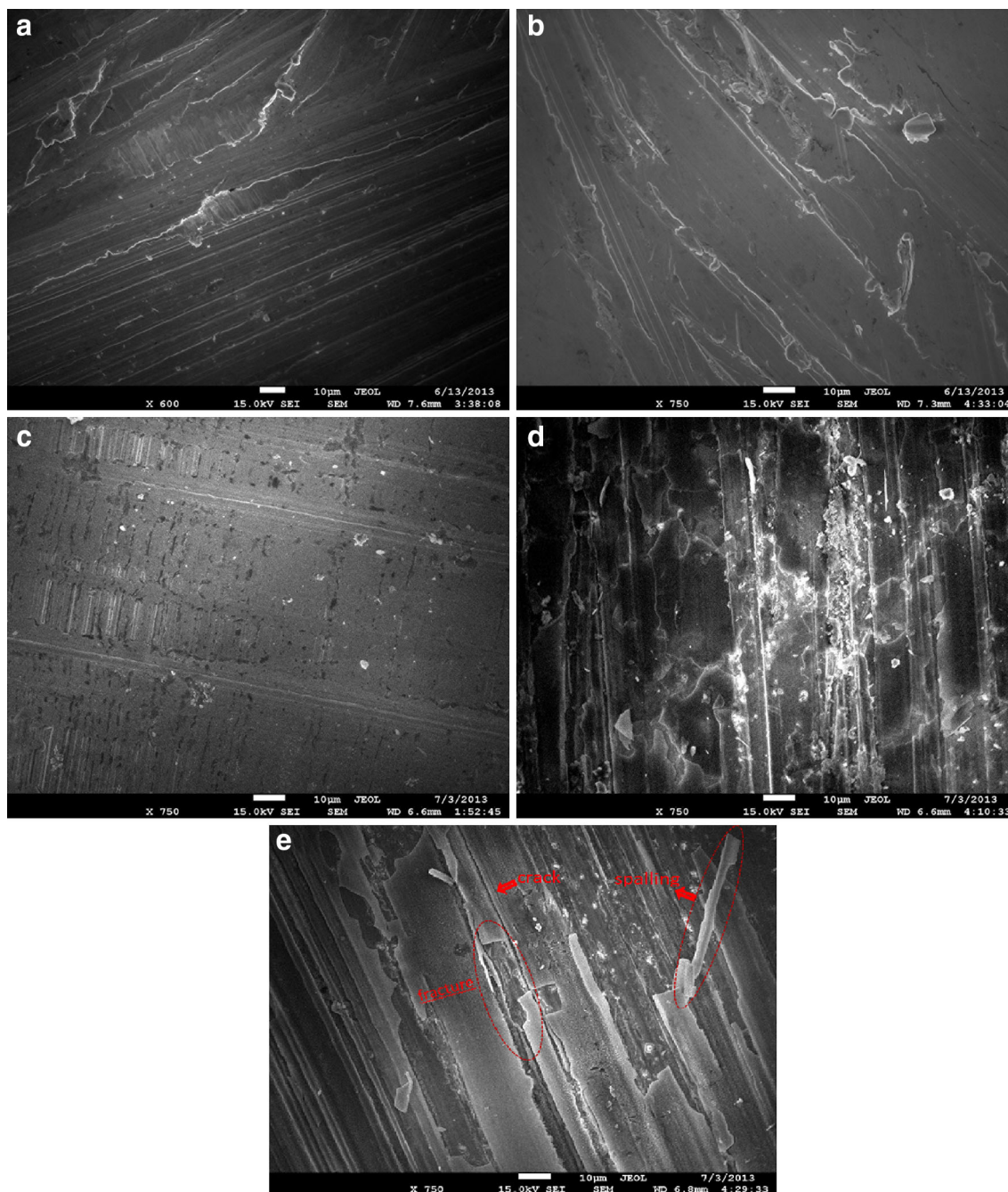


Fig. 5 SEM images of oxidized Cu–Al–Ni–Fe shape-memory alloy at, **a** 500 °C, **b** 600 °C, **c** 700 °C, **d** 800 °C and **e** 900 °C

analyses of the samples were performed (Fig. 4). The XRD pattern of the alloy oxidized at 500 °C for 1 h consists of two different phases. Among different peaks observed in the XRD plot, those at Bragg angles $2\theta = 42.82^\circ$, 44.28° and 49.84° were attributed to 18R martensite phase and the peak at $2\theta = 73.06^\circ$ was attributed to magnetite (Fe_3O_4) phase. In a previous study conducted by our group [21], Fe precipitates were observed in the Cu–Al–Ni–Fe alloy to which heat treatment was not applied. It is considered that Fe_3O_4

oxide phase in the alloy subjected to oxidation at 500 °C formed by oxidation of these precipitates. X-ray diffractometer pattern of the alloy given in Fig. 4b clearly shows that phase components present in the alloy changed with increasing oxidation temperature. While the intensities of peaks belonging to 18R martensite and Fe_3O_4 phases diminished, a new phase appeared on the surface of the alloy. This phase was aluminum oxide (Al_2O_3) and as a result of increasing oxidation temperature, number and

intensity of the peaks belonging to this phase increased, while intensity of peaks belonging to 18R martensite and Fe_3O_4 phases reduced significantly. These results point out that the surface of the alloy started to be covered by an Al_2O_3 layer at oxidation temperature of 800 °C.

X-ray diffractometer pattern of the alloy oxidized at 900 °C for 1 h is shown in Fig. 4. As a result of the high temperature oxidation, some of the peaks belonging to main phase 18R martensite disappeared ($2\theta = 44.28^\circ$ and 49.84°) and the intensity of the Fe_3O_4 phase peak decreased significantly. The peak with the maximum intensity ($2\theta = 46.58^\circ$) belongs to Al_2O_3 phase. This could be explained such that upon high-temperature oxidation, the surface of the alloy was covered by an Al_2O_3 layer while phases forming the main structure remained beneath this oxide layer. Additionally, coverage of the surface of the alloy by Al_2O_3 prevented the oxidation of Cu and Ni present in the alloy [18]. Meanwhile, in XRD plot, the reason of the significant reduction in the intensity of the Fe_3O_4 peak is the dissolution of most of the Fe precipitates in the matrix phase at high-oxidation temperatures [21]. Semi-quantitative phase analyses and surface morphology examinations of the samples were performed by obtaining their SEM images and EDX spectra. A low-magnification SEM image of the alloy oxidized at 500 °C showing the surface morphology of the sample is shown in Fig. 5a. Energy-dispersive X-ray analysis taken from the whole surface of the sample showed that the surface contained 4.61 wt% (14.06 at%) oxygen. Apart from this, cutting marks and martensite band structures on the surface of the samples could be seen clearly. As a result, oxidation performed at 500 °C did not yield a variation in the morphology of the surface of the alloy. Energy-dispersive X-ray analyses obtained from the surfaces of the alloy samples oxidized at 600 and 700 °C, which had similar morphological properties, showed that the amount of oxygen at the sample surfaces increased with increasing oxidation temperature. The amount of oxygen detected at the sample surfaces oxidized at 600 and 700 °C was ~ 6.04 wt% (~ 17.86 at%) and ~ 10.54 wt% (~ 27.69 at%), respectively. Additionally, results of the EDX spectra obtained from different regions of the alloy oxidized at 700 °C were consistent with results of the XRD plots given in Fig. 4c. Energy-dispersive X-ray point analyses demonstrated that Al_2O_3 oxide phase started to nucleate at the surface of the alloy.

Scanning electron microscope images of the samples oxidized at 800 and 900 °C are shown in Fig. 5d and e, respectively. The morphological changes on the surface of the alloy samples due to increasing oxidation temperature are clearly seen in the SEM images. Energy-dispersive X-ray analyses taken from the surfaces of the samples demonstrated that oxygen content at the surface of the samples increased with oxidation temperature. The oxygen

content of the surfaces of the alloy samples was found to be 23.26 wt% (46.01 at%) and 32.88 wt% (53.10 at%) for oxidation temperatures of 800 and 900 °C, respectively. Energy-dispersive X-ray point analyses taken from the surface of the samples indicated that the surface of the samples was mainly covered by an Al_2O_3 phase. These results show a perfect consistency with the XRD results given in Fig. 4d and e (the strongest peak in the XRD pattern given in Fig. 4e belongs to Al_2O_3). Additionally, if the SEM image of the alloy oxidized at 900 °C is examined in detail (Fig. 5e), cracks, fractures and spallings formed in the surface oxide layer of the sample can be observed. This could be attributed to the complete saturation of the surface of the alloy by oxygen at 900 °C as the oxidation parameter reached to a constant value at this temperature, indicating that complete saturation was attained (Fig. 2).

4 Conclusions

From this study, where isothermal oxidation behavior of a Cu–Al–Ni–Fe shape-memory alloy at high temperatures and the effect of this behavior on the structural and morphological properties of the alloy were investigated, the following conclusions can be drawn:

- Oxidation constant (K_p) was almost constant at low oxidation temperatures, such as 500 and 600 °C, while it increased with oxidation temperature. On the other hand, it can be stated that complete saturation of the alloy with oxygen was attained at the maximum oxidation temperature examined, i.e., 900 °C, as K_p value was almost constant at this temperature (Fig. 2)
- The activation energy for oxidation of Cu–Al–Ni–Fe alloy examined in this study was relatively higher than Cu–Al–Ni shape-memory alloys given in the literature. However, if this alloy is compared to non-heat-treated Ni-rich NiTi, it can be seen that activation energy of Cu–Al–Ni–Fe was lower. However, when compared to Ni–Ti alloys, the higher resistance of Cu–Al–Ni–Fe alloys to oxidation indicates that heat treatment could be applied to the latter rather easily.
- X-ray diffractometer analyses showed that high-temperature oxidation affects the structural properties of the Cu–Al–Ni–Fe alloy. With increasing oxidation temperature, number and intensity of the characteristic peaks belonging to 18R martensite phase were reduced, while those of Al_2O_3 phase were increased.
- Results obtained from SEM images and EDX spectra were highly consistent with those obtained from XRD analyses. Morphological examination of the samples showed that the surface morphology of the samples was comprised of mainly martensite phase at low oxidation

temperatures, while with increasing oxidation temperature, martensite structure disappeared and the surface was covered by an oxide layer. When the oxidation temperature reached 900 °C, cracks, fractures and spallings formed on the surface of the sample were observed.

Acknowledgments We acknowledge Dr. Selçuk Aktürk (Materials Research Lab., Mugla Sıtkı Kocman University) for the SEM–EDX observations and analyses. We also wish to thank Professor Yusuf Atıcı (Firat University) and Professor Yıldırım Aydoğdu (Gazi University) due to their helpful supporting.

References

1. K. Otsuka, X. Ren, Recent developments in the research of shape memory alloys. *Intermetallics* **7**, 511–528 (1999)
2. R. Zengin, Microstructure and oxidation properties of a neutron-irradiated Cu-13.5 wt% Al-4 wt% Ni shape memory alloy. *Phys. B* **363**, 110–114 (2005)
3. A. Planes, L. Mañosa, D. Ríos-Jara, J. Ortín, Martensitic transformation of Cu-based shape-memory alloys: elastic anisotropy and entropy change. *Phys. Rev. B* **45**, 7633–7639 (1992)
4. Y. Sutou, T. Omori, K. Yamauchi, N. Ono, R. Kainuma, K. Ishida, Effect of grain size and texture on pseudoelasticity in Cu–Al–Mn-based shape memory wire. *Acta Mater.* **53**, 4121–4133 (2005)
5. G. Lojen, M. Gojić, I. Anžel, Continuously cast Cu–Al–Ni shape memory alloy—properties in as-cast condition. *J. Alloy. Compd.* **580**, 497–505 (2013)
6. J.I. Pérez-Landazábal, V. Recarte, V. Sánchez-Alarcos, M.L. Nó, J.S. Juan, Study of the stability and decomposition process of the β phase in Cu–Al–Ni shape memory alloys. *Mater. Sci. Eng. A* **438**, 734–737 (2006)
7. P.P. Rodríguez, A. Ibarra, A. Iza-Mendia, V. Recarte, J.I. Pérez-Landazábal, J.S. Juan, M.L. Nó, Influence of thermo-mechanical processing on the microstructure of Cu-based shape memory alloys produced by powder metallurgy. *Mater. Sci. Eng. A* **378**, 263–268 (2004)
8. G.R. Wallwork, The oxidation of alloys. *Rep. Prog. Phys.* **39**, 401–485 (1976)
9. G.C. Wood, F.H. Stott, Oxidation of alloys. *Mater. Sci. Technol.* **3**, 519–529 (1987)
10. Z. Cao, Y. Shen, F. Li, L. Yu, Oxidation of a quaternary two-phase Cu-40 Ni-17.5 Cr-2.5 Al alloy at 973–1073 K in 101 kPa O₂. *J. Alloy. Compd.* **480**, 449–453 (2009)
11. B. Yujun, L. Chengwei, G. Guili, Y. Longwei, TEM observation of oxidation of CuZnAlMnNi shape memory alloy. *Chin. Sci. Bull.* **46**, 1837–1839 (2001)
12. Y.-J. Bai, Y.-X. Liu, D.-S. Sun, X.-F. Bian, L.-M. Xiao, G.-L. Geng, Atmospheric oxidation of CuZnAlMnNi shape memory alloy. *Mater. Lett.* **46**, 358–361 (2000)
13. B.I. Portillo, S.K. Varma, Oxidation behavior of Nb-20Mo-15Si-5B-20Ti alloy in air from 700 to 1300 °C. *J. Alloy. Compd.* **497**, 68–73 (2010)
14. C.H. Xu, X.Q. Ma, S.Q. Shi, C.H. Woo, Oxidation behavior of TiNi shape memory alloy at 450–750 °C. *Mater. Sci. Eng. A* **371**, 45–50 (2004)
15. M. Kök, G. Pirge, Y. Aydogdu, Isothermal oxidation study on NiMnGa ferromagnetic shape memory alloy at 600–1000 °C. *Appl. Surf. Sci.* **268**, 136–140 (2013)
16. C. Tatar, R. Zengin, The effects of neutron irradiation on oxidation behavior, microstructure and transformation temperatures of Cu-12.7 wt% Al-5 wt% Ni-2 wt% Mn shape memory alloy. *Thermochim. Acta* **433**, 56–58 (2005)
17. C. Tatar, R. Zengin, The effects of neutron irradiation on shape memory properties and oxidation behaviour of a Cu-13Al-4Ni alloy. *Int. J. Therm. Sci.* **47**, 899–902 (2008)
18. R. Zengin, S. Ozgen, M. Ceylan, Oxidation behaviour and kinetics properties of shape memory CuAl_xNi₄ ($x = 13.0$ and 13.5) alloys. *Thermochim. Acta* **414**, 79–84 (2004)
19. R.G. Reddy, X. Wen, M. Divakar, Isothermal oxidation of TiAl alloy. *Metall. Mater. Trans. A* **32**, 2357–2361 (2001)
20. F. Dagdelen, E. Ercan, The surface oxidation behavior of Ni-45.16% Ti shape memory alloys at different temperatures. *J. Therm. Anal. Calorim.* **115**, 561–565 (2014)
21. K. Yildiz, M. Kök, Study of martensite transformation and microstructural evolution of Cu–Al–Ni–Fe shape memory alloys. *J. Therm. Anal. Calorim.* **115**, 1509–1514 (2014)